

# Superhydrophobic Surfaces Prepared by Microstructuring of Silicon Using a Femtosecond Laser

Tommaso Baldacchini,<sup>†</sup> James E. Carey,<sup>†</sup> Ming Zhou,<sup>†,‡</sup> and Eric Mazur<sup>\*,†</sup>

Division of Engineering and Applied Sciences, Harvard University, 29 Oxford Street, Cambridge, Massachusetts 02138, and School of Materials Science and Engineering, Jiangsu University, 301 Xuefu, Zhenjiang, Jiangsu 212013, PRC

Received December 13, 2005. In Final Form: March 31, 2006

We present a simple method for fabricating superhydrophobic silicon surfaces. The method consists of irradiating silicon wafers with femtosecond laser pulses and then coating the surfaces with a layer of fluoroalkylsilane molecules. The laser irradiation creates a surface morphology that exhibits structure on the micro- and nanoscale. By varying the laser fluence, we can tune the surface morphology and the wetting properties. We measured the static and dynamic contact angles for water and hexadecane on these surfaces. For water, the microstructured silicon surfaces yield contact angles higher than 160° and negligible hysteresis. For hexadecane, the microstructuring leads to a transition from nonwetting to wetting.

## Introduction

Superhydrophobic surfaces exhibit contact angles ( $\theta$ ) with water that are larger than 150° and a negligible difference  $\Delta\theta$  between the advancing and receding contact angles, the so-called contact angle hysteresis.<sup>1,2</sup> An example of a naturally occurring superhydrophobic surface is the lotus leaf. Upon landing on the surface of a lotus leaf, water beads up to form nearly spherical drops that immediately roll off.<sup>3,4</sup> Synthetic superhydrophobic surfaces have attracted considerable attention because of their potential application in devices where contact with water is detrimental to performance or durability.<sup>5,6</sup> The decreased contact area between water and solid surfaces in superhydrophobic samples reduces effects such as friction, erosion, and contamination.

The wettability of a surface depends on both its chemical nature and topology. Although lowering the surface energy of a substrate decreases its wettability, contact angles larger than 120° have never been achieved for water on flat surfaces.<sup>7</sup> Inspired by the topology of the lotus leaf, researchers devised methods for roughening surfaces with low surface energies to achieve the high contact angles and low contact angle hysteresis necessary for superhydrophobicity.<sup>8</sup> Some of the numerous approaches employed in the preparations of superhydrophobic surfaces include lithographically patterned substrates,<sup>9,10</sup> vertically aligned carbon nanotubes,<sup>11,12</sup> anodically oxidized metal surfaces,<sup>13,14</sup> polyelectrolyte layers,<sup>15</sup> block copolymers,<sup>16,17</sup> sublimation,<sup>18,19</sup> and nanocasting and extruding of polymers.<sup>20,21</sup> Here, we present a novel and simple structuring process that uses intense femtosecond laser pulses to create microstructured superhydrophobic surfaces with remarkable wetting characteristics.

## Experimental Section

Previously, we reported on the fabrication of arrays of conical micrometer-sized spikes by irradiating silicon surfaces with femtosecond laser pulses.<sup>22–25</sup> For the experiments described here, we used *n*-doped Si(100) wafers ( $\rho = 1 \Omega/\text{m}$ ). Each silicon wafer was cleaned with a 15-min ultrasonic bath in trichloroethylene, followed by a 15-min ultrasonic bath in acetone, and finally a 15-min ultrasonic bath in methanol. After drying the silicon substrates in a nitrogen gas flow, they were transferred to a magnetizable sample holder mounted onto a two-axis computer-controlled stage inside a processing chamber that was filled with SF<sub>6</sub> at a pressure of 0.67 × 10<sup>4</sup> Pa.

We use a regeneratively amplified Ti:sapphire laser system that generates a train of 100-fs laser pulses at a repetition rate of 1 kHz. The laser pulses have a center wavelength of 800 nm and energies up to 400 μJ. The laser pulses are focused at normal incidence onto the silicon sample using a 250-mm focal length, antireflection-coated, plano-convex lens mounted on a single-axis linear translation stage. By moving the lens and therefore the position of the focus, the diameter of the laser spot size at the sample surface can be varied from 30 to 250 μm. To structure an area larger than the laser spot size, the silicon substrate was translated relative to the laser beam, exposing any given spot on the silicon surface to an average of 200 pulses.

(11) Lau, K. K. S.; Bico, J.; Teo, K. B. K.; Chhwalla, M.; Amaratunga, G. A. J.; Milne, W. I.; McKinley, G. H.; Gleason, K. K. *Nano Lett.* **2003**, *3*, 1701.

(12) Li, H.; Wang, X.; Song, Y.; Liu, Y.; Li, Q.; Jiang, L.; Zhu, D. *Angew. Chem., Int. Ed.* **2001**, *40*, 1743.

(13) Tsujii, K.; Yamamoto, T.; Onda, T.; Shibuichi, S. *Angew. Chem., Int. Ed.* **1997**, *36*, 1011.

(14) Shibuichi, S.; Yamamoto, T.; Onda, T.; Tsujii, K. *J. Colloid Interface Sci.* **1998**, *208*, 287.

(15) Zhai, L.; Cebeci, F. Ç.; Cohen, R. E.; Rubner, M. F. *Nano Lett.* **2004**, *4*, 1349.

(16) Xie, Q.; Fan, G.; Zhao, N.; Guo, X.; Xu, J.; Dong, J.; Zhang, L.; Zhang, Y.; Han, C. C. *Adv. Mater.* **2004**, *16*, 1830.

(17) Han, J. T.; Xu, X.; Cho, K. *Langmuir* **2005**, *21*, 6662.

(18) Nakajima, A.; Fujishima, A.; Hashimoto, K.; Watanabe, T. *Adv. Mater.* **1999**, *11*, 1365.

(19) Miwa, M.; Nakajima, A.; Fujishima, A.; Hashimoto, K.; Watanabe, T. *Langmuir* **2000**, *16*, 5754.

(20) Feng, L.; Li, S.; Li, H.; Zhai, J.; Song, Y.; Jiang, L.; Zhu, D. *Angew. Chem., Int. Ed.* **2002**, *41*, 1221.

(21) Feng, L.; Song, Y.; Zhai, J.; Liu, B.; Xu, J.; Jiang, L.; Zhou, D. *Angew. Chem., Int. Ed.* **2003**, *42*, 800.

(22) Her, T.-H.; Finlay, R. J.; Wu, C.; Deliwala, S.; Mazur, E. *Appl. Phys. Lett.* **1998**, *73*, 1673.

(23) Her, T.-H.; Finlay, R. J.; Wu, C.; Mazur, E. *Appl. Phys. A* **2000**, *70*, 383.

(24) Crouch, C. H.; Carey, J. E.; Shen, M.; Mazur, E.; Génin, F. Y. *Appl. Phys. A* **2004**, *79*, 1635.

(25) Sheehy, M. A.; Wilson, L.; Carey, J. E.; Friend, C. M.; Mazur, E. *Chem. Mater.* **2005**, *17*, 3582.

\* Corresponding author. E-mail: mazur@physics.harvard.edu.

<sup>†</sup> Harvard University.

<sup>‡</sup> Jiangsu University.

(1) Chen, W.; Fadeev, A. Y.; Hsieh, M. C.; Öner, D.; Youngblood, J.; McCarthy, T. J. *Langmuir* **1999**, *15*, 3395.

(2) Feng, L.; Li, S.; Li, Y.; Li, H.; Zhang, L.; Zhai, J.; Song, Y.; Liu, B.; Jiang, L.; Zhu, D. *Adv. Mater.* **2002**, *14*, 1857.

(3) Barthlott, W.; Neinhuis, C. *Planta* **1997**, *202*, 1.

(4) Neinhuis, C.; Barthlott, W. *Ann. Bot.* **1997**, *79*, 667.

(5) Blossey, R. *Nat. Mater.* **2003**, *2*, 301.

(6) Nakajima, A.; Hashimoto, K.; Watanabe, T. *Monatsh. Chem.* **2001**, *132*, 31.

(7) Nishino, T.; Meguro, M.; Nakamae, K.; Matsushita, M.; Ueda, Y. *Langmuir* **1999**, *15*, 4321.

(8) Sun, T.; Feng, L.; Gao, X.; Jiang, L. *Acc. Chem. Res.* **2005**, *38*, 644.

(9) Öner, D.; McCarthy, T. J. *Langmuir* **2000**, *16*, 7777.

(10) Fürstner, R.; Barthlott, W.; Neinhuis, C.; Walzel, P. *Langmuir* **2005**, *21*, 956.

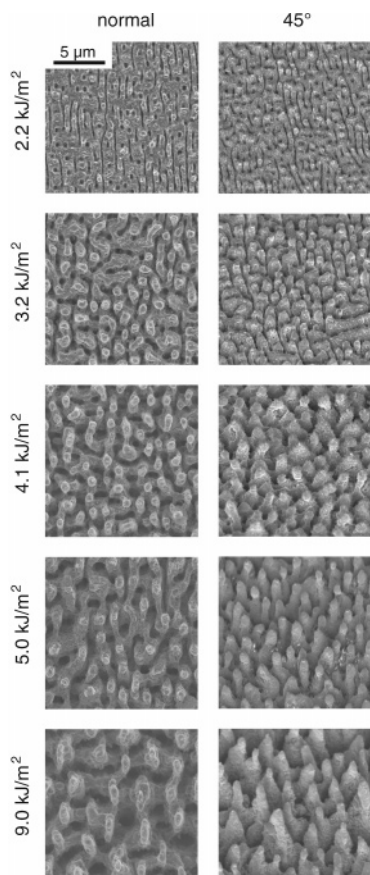


**Figure 1.** Top and side view ( $45^\circ$ ) scanning electron micrographs of silicon surfaces microstructured in  $\text{SF}_6$  at various laser fluences.

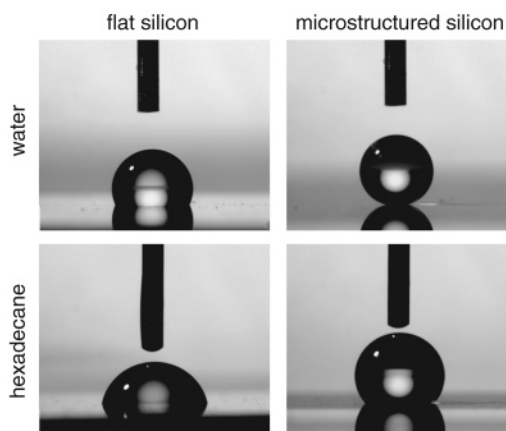
Following laser irradiation, the microstructured silicon surfaces were treated for 60 s in air plasma. Immediately afterward, the samples were exposed to (heptadecafluoro-1,1,2,2-tetrahydrodecyl)trichlorosilane ( $\text{CF}_3(\text{CF}_2)_7\text{CH}_2\text{CH}_2\text{SiCl}_3$ ) for 3 h in a low-pressure chamber. The same surface treatment was used for the flat silicon samples that were not microstructured.

We determined the static contact angles for water and hexadecane by the sessile drop method with a contact angle meter and averaged over five measurements. We used  $5\text{-}\mu\text{L}$  droplets for all experiments. The contact angle hysteresis was measured by tilting the sample using a goniometer.

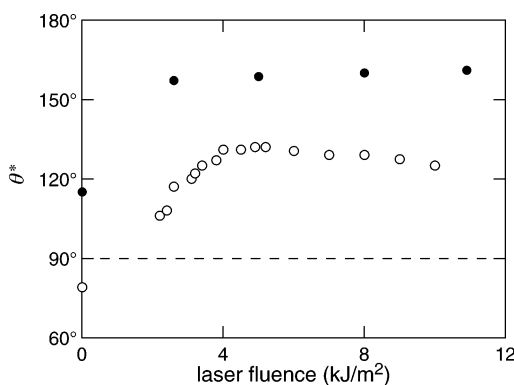
## Results

Figure 1 shows a sequence of scanning electron microscopy pictures of microstructured silicon surfaces made with several incident laser fluences and a constant average shot number (200 pulses/area). The morphology of the structured sample changes dramatically in the range of fluence from 2.2 to  $9.0\text{ kJ/m}^2$ ; the surface topology goes from laser-induced periodic surface structures to a coarsened surface to an array of cone-shaped spikes.<sup>23,24</sup> No microstructuring is observed for fluences lower than  $2\text{ kJ/m}^2$ . Shallow wavy ridges are formed at fluences between 2 and  $3.5\text{ kJ/m}^2$ . Separated protrusions with larger aspect ratios begin to appear at  $4.0\text{ kJ/m}^2$ ; well-defined conical-shaped spikes are observable with increasing fluence. The base of each spike has an asymmetric shape, with the short axis of the base always parallel to the laser polarization. An important trend to notice in Figure 1 is that with increasing fluence there is an increase in both the microstructure height and the distance between microstructures.

After laser microstructuring, the sample surface is treated in air plasma to clean the surface and oxidize it and then terminated with fluorosilane. Fluorosilane termination lowers the surface



**Figure 2.** Photographs of water (top) and hexadecane (bottom) droplets on flat (left) and microstructured (right) silicon surfaces treated with fluorosilane. The same silicon surface, microstructured at a laser fluence of  $8.0\text{ kJ/m}^2$ , was used for the two pictures on the right.



**Figure 3.** Static contact angles of water (●) and hexadecane (○) on microstructured silicon surfaces as a function of microstructuring laser fluence. The values on the vertical axis at zero laser fluence are for the native silicon substrate. All surfaces were treated with fluorosilane.

energy<sup>7</sup> and allows us to study the hydrophobic effect of roughness imparted by the laser structuring. Figure 2 shows images of water droplets on flat and microstructured silicon surfaces, respectively. In both cases, the surface has been terminated with fluorosilane. The contact angle on the flat surface is  $115^\circ$ , but on the microstructured surface, the contact angle is  $160^\circ$ , an increase of  $45^\circ$ .

Figure 3 shows how the contact angle depends on the laser fluence used for microstructuring the silicon surface. The data points at zero fluence were obtained on unstructured (i.e., flat) silicon surfaces. For water, the contact angle increases by  $40^\circ$  upon microstructuring with a minimum fluence of  $2.6\text{ kJ/m}^2$  but then remains nearly constant, independent of the laser fluence, even though the morphology of the sample surfaces varies significantly between 2 and  $4\text{ kJ/m}^2$ . The wetting properties of these surfaces are very stable; a sample with a laser fluence of  $8\text{ kJ/m}^2$  maintained the same high contact angle ( $160^\circ$ ) after being completely immersed in water for one week.

We also measured the contact angle for hexadecane on the microstructured silicon surfaces. Because hexadecane has a lower surface tension than water ( $\gamma_{\text{H}_2\text{O}} = 72.0\text{ mN/m}$ ;  $\gamma_{\text{HD}} = 26.7\text{ mN/m}$ ),<sup>26</sup> it wets more of the microstructured silicon surfaces and therefore exhibits lower contact angles than water. Figure 2 shows images of hexadecane droplets on fluorosilane-terminated flat and microstructured silicon surfaces. It is interesting that whereas hexadecane wets the flat surface ( $\theta < 90^\circ$ ) it does not

**Table 1. Contact Angle Hysteresis ( $\Delta\theta$ ) for Water and Hexadecane on Silicon Surfaces Microstructured with Different Laser Fluences (Incident Energy per Unit Area)<sup>a</sup>**

fluence (kJ/m <sup>2</sup> )	$\Delta\theta_{\text{water}}$	$\Delta\theta_{\text{hexadecane}}$
2.6	30°	22°
5.0	<3°	29°
8.0	<3°	23°
10.9	<3°	33°

<sup>a</sup> All surfaces were treated with a fluorosilane agent after microstructuring.

wet the microstructured surface ( $\theta > 90^\circ$ ). The empty circles in Figure 3 represent the dependence of the contact angle of hexadecane on laser fluence. The contact angle increases by 30° upon microstructuring with a minimum fluence of 2.6 kJ/m<sup>2</sup>. In contrast to water, however, the laser fluence has a significant effect on the contact angles for hexadecane. The contact angle increases as the laser fluence is increased from 2.2 to 4.5 kJ/m<sup>2</sup> and then begins to decrease. The microstructuring changes the contact angle from a wetting value of 79° on flat silicon to a nonwetting value between 105 and 129° on the laser-microstructured surface.

Superhydrophobic surfaces exhibit not only contact angles greater than 150° but also small contact angle hysteresis—that is, there is little or no difference between the advancing and receding contact angles. We measured contact angle hysteresis by means of a goniometer that allows tilting of the microstructured substrate (Table 1). Droplets of water on silicon surfaces microstructured at a fluence larger than 5.0 kJ/m<sup>2</sup> roll off immediately at the smallest tilting angle (<2°). For these fluences, the microstructured surfaces meet the criteria for a superhydrophobic surface. At a fluence of 2.6 kJ/m<sup>2</sup>, we find a contact angle hysteresis of 30°. In contrast to water, hexadecane exhibits a large contact angle hysteresis for all microstructuring fluences.

### Discussion

Nearly seven decades ago, two models were proposed to describe the effects of surface roughness on hydrophobicity.<sup>27,28</sup> In the Wenzel model,<sup>27</sup> the liquid is assumed to be in contact with every part of the rough surface, and the increase in contact angle is simply a result of the increase in surface area. Wenzel proposed that the contact angle,  $\theta^*$ , on the roughened surface is given by<sup>27</sup>

$$\cos \theta^* = r \cos \theta \quad (1)$$

where  $r$  is the ratio between the actual and projected surface areas and  $\theta$  is the contact angle measured on the equivalent flat surface. Because  $r$  is always greater than 1, this model predicts that the contact angle of a liquid that wets a surface ( $\theta < 90^\circ$ ) always decreases when that surface is roughened ( $\theta^* < \theta$ ). Likewise, the contact angle of a liquid that does not wet the surface ( $\theta > 90^\circ$ ) always increases when that surface is roughened ( $\theta^* > \theta$ ). Indeed, roughening a nonwetting surface increases its hydrophobicity.<sup>10,11</sup>

In contrast, the Cassie–Baxter model<sup>28</sup> assumes that the liquid does not completely wet the roughened substrate. Air pockets are trapped in the crevices of the rough surface, and the liquid interacts with the composite surface made of substrate material and air. In this configuration, the measured contact angle on a roughened surface ( $\theta^*$ ) is given by<sup>28</sup>

$$\cos \theta^* = -1 + \phi_s(1 + \cos \theta) \quad (2)$$

where  $\phi_s$  represents the fraction of the solid in contact with

liquid and  $\theta$  is the contact angle measured on the equivalent flat surface. The smaller the value of  $\phi_s$ , the smaller the contact area between the solid and the liquid and the larger the increase in the measured contact angle. Because  $\phi_s$  is less than 1, the Cassie–Baxter model always predicts an increase in  $\theta^*$ , independent of the value of  $\theta$ .

The very low contact angle hysteresis we observe for water on surfaces microstructured at high fluence are consistent only with the Cassie–Baxter model. The micrometer-scale spikes break the three-phase (solid–liquid–air) contact line of the water droplet, causing it to destabilize.<sup>9,29</sup> The small contact area between water and the tip of the silicon spikes results in a small  $\phi_s$  in eq 2 and gives rise to a large contact angle  $\theta^*$ , allowing the water droplet to roll off the microstructured silicon surface easily. The topology of samples microstructured with less than 5 kJ/m<sup>2</sup> results in different behavior. As can be seen in Figure 1, the surface of the low-fluence samples is not covered with individual micrometer-scale spikes but a nearly continuous network of ridges. The three-phase contact line of a water droplet on this type of surface is more stable, so the water droplet is “pinned” more easily. Although these low fluence samples exhibit a large static contact angle, the contact angle hysteresis indicates that they are not truly superhydrophobic.

The observed transition for hexadecane from a contact angle below 90° to a contact angle above 90° as a result of surface roughening is also consistent with the Cassie–Baxter model. In contrast to water, however, hexadecane exhibits rather large contact angle hysteresis even at laser fluences where the surface is covered with many micrometer-scale spikes. This difference in behavior can be attributed to the smaller contact angle of hexadecane on both flat and microstructured silicon compared to that of water. Substituting the contact angles for a surface fabricated at a laser fluence of 8 kJ/m<sup>2</sup> into eq 2, we obtain  $\phi_s = 0.3$  for hexadecane and  $\phi_s = 0.1$  for water. Because a larger fraction  $\phi_s$  of the silicon surface is in contact with hexadecane, hexadecane droplets are more easily pinned than water droplets, explaining the observed large contact angle hysteresis for hexadecane.

### Conclusions

We fabricated superhydrophobic silicon surfaces using femtosecond-laser microstructuring. For water, we observe contact angles greater than 160° with negligible hysteresis. We examined the dependence on laser fluence of the static and dynamic wetting properties of these surfaces for both water and hexadecane and found that the behavior of both liquids follows the Cassie–Baxter model. The morphology of the microstructured areas can easily be controlled, allowing for the design of silicon surfaces with different wetting properties. The simplicity of the technique and the convenient control of the resulting wetting properties make laser-microstructured silicon an attractive substrate for many applications.

**Acknowledgment.** This research was supported by the Army Research Office under award no. W911NF-05-1-0341. We thank Professor M. F. Rubner and Dr. X. Shen for their assistance with contact angle measurements. We thank Professor H. A. Stone, Dr. R. Shalek, Dr. D. B. Wolfe, and J. Kriebel for helpful discussions.

LA053374K

(26) Laibinis, P. E.; Bain, C. D.; Nuzzo, R. G.; Whitesides, G. M. *J. Phys. Chem.* **1995**, *99*, 7663.

(27) Wenzel, R. N. *Ind. Eng. Chem.* **1936**, *28*, 988.

(28) Cassie, A. B. D.; Baxter, S. *Trans. Faraday Soc.* **1944**, *40*, 546.

(29) Shang, H. M.; Wang, Y.; Takahashi, K.; Cao, G. Z.; Li, D.; Xia, Y. N. *J. Mater. Sci.* **2005**, *40*, 3587.